A comparative study on the structural properties of ZnO and Ni-doped ZnO nanostructures

Kyung Ho Kim[*], Zhuguang Jin, Yoshio Abe, Midori Kawamura

Department of Materials Science and Engineering, Kitami Institute of Technology, 165

Koen-cho, Hokkaido 090-8507, Japan

Abstract

We investigated the structural properties of zinc oxide (ZnO) nanorods with various Ni

doping amounts. The length and diameter of the nanorods decreased and increased,

respectively, with increasing Ni doping amount to 5 mM. Ni-doped ZnO (Ni-ZnO)

nanorods exhibited better crystalline quality than undoped ZnO nanorods. In the visible

wavelength region, the optical transmittance of Ni-ZnO nanorods was slightly lower

than that of ZnO nanorods. Upon further increasing the Ni doping amount (7 mM), the

morphology of Ni-ZnO dramatically changed from that of nanorods to a sphere-like

structure assembled with interwoven nanowalls. Ni incorporation is a facile strategy for

tuning growth behavior and morphology of ZnO nanostructures.

Corresponding author: Kyung Ho Kim, Tel: 81-157-26-9431, Fax: 81-157-26-4973,

E-mail address: khkim@mail.kitami-it.ac.jp

1. Introduction

Zinc oxide (ZnO) nanostructures have become one of the most attractive candidates for the fabrication of nanoscale devices [1,2]. Therefore, it has become important to systematically study ZnO nanostructures with different dopants, as doping is a critical key parameter for tuning the physical properties of such nanostructures [2-4].

In our previous study, we fabricated Cu-, Ag-, and Al-doped ZnO nanorods, and investigated their structural and optical properties. Compared with undoped ZnO, the nanorod length increased with the incorporation of Cu, whereas it showed quite the opposite behavior with the incorporation of Ag. Moreover, the addition of Al resulted in a significant morphological change by transforming the nanorods to microrods [5].

Studies on Ni-doped ZnO (Ni-ZnO) nanostructures prepared by sputtering, precipitation, and spray pyrolysis methods have also been reported [6-12]. However, the structural properties of Ni-ZnO nanostructures fabricated using chemical solution deposition (CSD) on a fluorine-doped tin oxide (FTO)-coated glass substrate have rarely been described. CSD is a very convenient, simple, and inexpensive method [13]. Growth of nanostructures on a transparent conductive oxide (TCO) substrate is important for the formation of ZnO-based optoelectronic devices. In this study, we investigated the structural properties of Ni-ZnO nanostructures with various Ni doping

amounts and compared them with undoped ZnO nanorods.

2. Experimental

Prior to nanorod growth, 35-nm-thick ZnO seed layers were prepared on an FTO-coated glass substrate by using the sol-gel spin-coating method. The details of the fabrication process are described in our previous study [14].

Undoped ZnO nanorods were grown on the ZnO seed layers by using an aqueous solution of zinc acetate dihydrate ($Zn(CH_3COO)_2·2H_2O$, Sigma-Aldrich, 10 mM) and hexamethylenetetramine (HMT) ($C_6H_{12}N_4$, Sigma-Aldrich, 10 mM). For Ni-ZnO samples, nickel acetate tetrahydrate ($Ni(CH_3COO)_2·4H_2O$, Sigma-Aldrich, 1-7 mM) was added as a dopant in the solution. The seed layers were vertically kept in the solution at 90 ºC for 6 h; they were then washed with deionized water and dried at 120 ºC for 10 min.

The crystalline phase and orientation of the ZnO and Ni-ZnO samples were examined by performing X-ray diffraction (XRD, Bruker, D8 ADVANCE) measurement with Cu Kα radiation (λ = 0.15406 nm). The surface morphology and chemical compositions of the samples were investigated by field emission scanning electron microscope (FESEM) (JEOL, JSM-6701F) attached with an energy dispersive

X-ray spectroscopy (EDX) instrument. Optical transmittance spectra of the samples were obtained using ultraviolet-visible (UV-vis) spectroscopy (HITACHI, U-2910).

3. Results and discussion

Fig. 1 shows the XRD patterns of ZnO, 1 mM and 5 mM Ni-ZnO samples. All peaks are attributed to the hexagonal wurtzite phase of ZnO (JCPDS card No. 36-1451). No impurity peaks corresponding to Zn, Ni, and NiO are observed. The peak intensity of the (002) plane increases with an increase of Ni doping amount to 5 mM, indicating that the crystalline quality of the nanorods enhances. Details about the diffraction peak position and lattice parameters are listed in Table S1 in Supporting Information. Upon incorporation of Ni, the peak positions of (100), (002), (101), and (102) shift toward higher angles, indicating that Ni ions substitute Zn ions in the ZnO lattice owing to the slight difference between the ionic radii of Ni^{2+} (0.069 Å) and Zn^{2+} (0.74 Å) [15]. The lattice constants a and c of ZnO decrease from 3.2489 Å and 5.2035 Å to 3.2470 Å and 5.1977 Å, respectively, with incorporation of 5 mM Ni.

Fig. 2 shows the FESEM images of ZnO (a,b), 1 mM (c,d), and 5 mM (e,f) Ni-ZnO nanorods grown on ZnO seed layers prepared on FTO-coated glass substrates. The cross-sectional views show that all nanorods samples are uniformly distributed and

vertically well-aligned on the substrates. Top-view images reveal that the nanorods are hexagonal-shaped regardless of Ni doping. The Ni doping amount calculated by EDX is 0.02 and 0.23 at.% for 1 mM and 5 mM Ni-ZnO (see Table S2), which is within the substitution limit of Ni in ZnO [13,16]. The length, diameter, and surface density of the nanorods with various Ni doping amounts are listed in the Table 1 (see Fig. S1). It is found that the length and surface density of the nanorods decrease with increasing Ni doping amount. However, the diameter increases with an increase in Ni amount. The aspect ratio of 5 mM Ni-ZnO is 9, which is considerably less compared to that of ZnO (34). Ni incorporation might have played a role in lowering the surface energy difference between polar and nonpolar surfaces, which hindered vertical growth and enhanced lateral growth [13,17].

The optical properties of the ZnO, 1 mM and 5 mM Ni-ZnO nanorods are shown in Fig. 3(a,b). In the visible region, the average transmittance of ZnO, 1 mM and 5 mM Ni-ZnO are 78, 76, and 72 %, respectively, as shown in Fig. 3(a). With Ni incorporation, the absorption edge of Ni-ZnO is slightly red-shifted [18]. The optical band gap (E_g) is estimated from the plot of photon energy versus $(\alpha h \upsilon)^2$, as shown in Fig. 3(b). The E_g values for ZnO, 1 mM and 5 mM Ni-ZnO are 3.29, 3.28 and 3.25 eV, respectively. The red shift of the band gap confirms the substitution of Ni in the ZnO lattice, which is

consistent with the XRD and SEM results [18].

Further increasing the Ni doping amount to 7 mM, the morphology of the nanorods is significantly changed. The cross-sectional and top-view of FESEM images of 7 mM Ni-ZnO are shown in Fig. 4(a,b), respectively. The Ni content is 8.87 at.% as determined by EDX (Table S2), which is beyond the substitution limit of Ni in the ZnO lattice [13,16]. The 7 mM Ni-ZnO sample has sphere-like structures assembled by interwoven nanowalls, which are randomly scattered on the substrate surface (Fig. S2). The diameter of the sphere and thickness of the nanowalls are ~3 μm and ~25 nm, respectively. The surface density of the spheres is ~0.01 μm^{-2}. It is worth noting that nanorods with a diameter of several nanometer are not observed on the substrate surface. The XRD pattern of 7 mM Ni-ZnO is shown in Fig. S3. Weak XRD peaks at (100), (002), and (101) planes of ZnO are observed owing to the low surface density of the sphere-like structures on the substrate surface. Unlike others, there is no preferential orientation. As shown in Fig. 4(c), 7 mM Ni-ZnO sample has good transparency in the visible region (see Fig. S4).

4. Conclusions

The effects of Ni doping amount on the structural properties of ZnO nanostructures

were investigated. Up to a certain amount (5 mM, within the substitution limit of Ni in ZnO), Ni-ZnO nanorods showed a typical hexagonal wurtzite structure with good crystalline quality. The diameter of the nanorods increased with an increase in the Ni doping amount, whereas their length and surface density decreased. The transmittance of the 1 mM and 5 mM Ni-ZnO nanorods was slightly lower than that of the ZnO nanorods. Beyond the substitution limit, 7 mM Ni-ZnO sample had sphere-like structure assembled by interwoven nanowalls. The amount of Ni doping plays a key role in the growth rate and surface morphology of ZnO nanostructures.

Figure captions

Fig. 1. XRD patterns of ZnO (a), 1mM (b) and 5 mM (c) Ni-ZnO samples on the FTO

substrates. Peaks related to the FTO substrate are labeled with rectangular.

Fig. 2. Cross-sectional (a,c,e) and top-view (b,d,f) FESEM images of ZnO (a,b), 1 mM

(c,d) and 5 mM (e,f) Ni-ZnO nanorods.

Fig. 3. Optical transmittance spectra (a) and plots of $(\alpha h\nu)^2$ versus $h\nu$ (b) of ZnO, 1mM

and 5 mM Ni-ZnO nanorods.

Fig. 4. Cross-sectional (a) and top-view (b) FESEM images and optical transmittance

spectrum (c) of 7 mM Ni-ZnO sample.

References

[1] A.B. Djurišić, X. Chen, Y.H. Leung, A.M-C. Ng, J. Mater. Chem. 22 (2012) 6526-6535.

[2] S.Y. Bae, C.W. Na, J.H. Kang, J. Park, J. Phys. Chem. B 109 (2005) 2526-2531.

[3] T-H. Fang, S-H. Kang, J. Appl. Phys. 105 (2009) 113512-1-113512-8.

[4] R. Jothi Ramalingam, G.S. Chung, Mater. Lett. 68 (2012) 247-250.

[5] K.H. Kim, Z. Jin, Y. Abe, M. Kawamura, Superlattice. Microst. 75 (2014) 455-460.

[6] R. Siddheswaran, J. Savková, R. Medlín, Jan Očenášek, O. Životský, P. Novak, P. Šutta, Appl. Surf. Sci. 316 (2014) 524-531.

[7] K. Raja, P.S. Ramesh, D. Geetha, Spectrochim Acta A 120 (2014) 19-24.

[8] T. Jan, J. Iqbal, M. Ismail, Q. Mansoor, A. Mahmood, A. Ahmad, Appl. Surf. Sci. 308 (2014) 75-81.

[9] N. Goswami, A. Sahai, Mater. Res. Bull. 48 (2013) 346-351.

[10] X. Chu, X. Zhu, Y. Dong, T. Chen, M. Ye, W. Sun, J. Electroanal. Chem. 676 (2012) 20-26.

[11] J. Zhao, L. Wang, X. Yan, Y. Yang, Y. Lei, J. Zhou, Y. Huang, Y. Gu, Y. Zhang, Mater. Res. Bull. 46 (2011) 1207-1210.

[12] S. Yilmaz, E. McGlynn, E. Bacaksiz, J. Cullen, R.K. Chellappan, Chem. Phys. Lett.

525-526 (2012) 72-76.

[13] S.H. Chiu, J.C.A. Huang, J. Non-Cryst. Solids 358 (2012) 2453-2457.

[14] K.H. Kim, Z. Jin, Y. Abe, M. Kawamura, Superlattice. Microst. 77 (2015) 101-107.

[15] R.D. Shannon, Acta Cryst. A 32 (1976) 751-767.

[16] G. Bulun, A. Ekicibil, S.K. Cetin, S. Demirdis, A. Coskun, K. Kiymac, J. Optoelectron. Adv. Mater. 13 (2011) 231-236.

[17] B. Meyer, D. Mark, Phys. Rev. B 67 (2003) 039902.

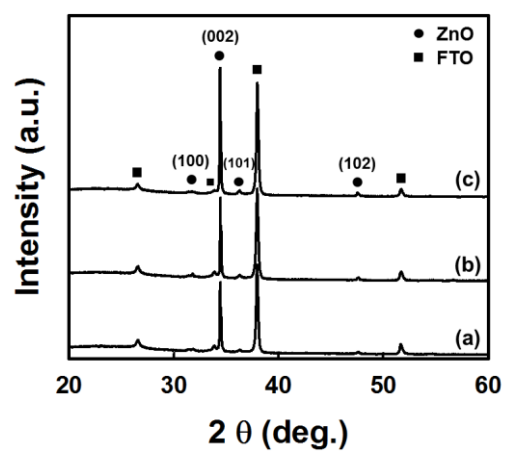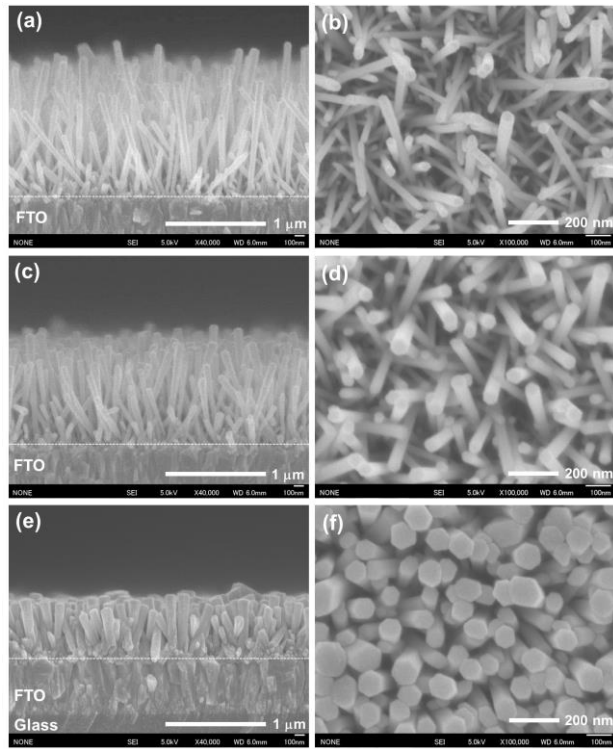[18] S. Venkataprasad Bhat, F.L. Deepak, Solid State Commun. 135 (2005) 345-347.
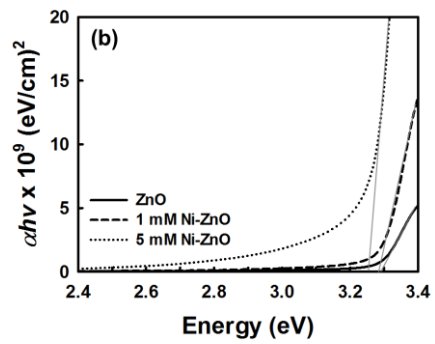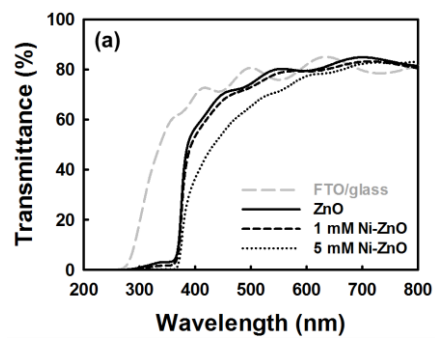
Fig. 1.

Fig. 2.

Fig. 3.

Fig. 4.